Oscillatory Rheometry Procedures for Highly Loaded Suspensions

Accounting for Retained Normal Force When Measuring Linear Moduli and Yield Stress

1. Introduction

Highly loaded suspension applications have emerged throughout industry in the 20th and 21st century as scientists and engineers have increasingly sought to incorporate fillers into polymeric binders to attain functional materials tailored to specific applications. These suspensions are defined as having greater than 50% of their volume occupied by solid additives [1]. By adding different fillers for varying applications these suspensions may be custom-built to achieve specific performance benefits. However, as more solids are added the physics of the resultant suspension becomes increasingly non-Newtonian, exhibiting yield stress and/or thixotopic behaviors. Further, these behaviors present a host of challenges that make both industrial processing and rheological evaluation non-trivial, among them: wall slip, edge fracture, binder separation, gap exudation, and local heterogeneity [2].

To take advantage of the performance benefits of highly loaded suspensions in manufacturing, these behaviors must first be overcome in rheological measurement [3,4]. Upon successfully establishing the ability to measure the material under various manufacturing-relevant processing conditions, the material can be characterized and the process tailored to its behavior. The most versatile tool for this characterization is the parallel plate rotational rheometer. This instrument can be used in steady torque mode, to measure viscosity, or in oscillatory torque mode, to measure visco-elastic behavior [5,6]. Both are critical to understanding the material characteristics and the requisite processing parameters [7]. Although engineers may have rheometers, a material to measure, and a desire to measure the properties of that material, the procedure for gathering quality data is not straightforward. It is openly accepted that the preparation and test parameters can affect the final measurement [7,14,24]. This poses a certain risk not only to the transferrability of knowledge to the manufacturing process but to the exchange of processes and procedures between researchers at different locations. Thus, there is a clear need for the detailing of a reasoned procedure for gathering visco-elastic data on highly loaded suspensions. Specifically of interest are the linear storage modulus (G'_{LVR}), the linear loss modulus (G''_{LVR}), and the yield stress (τ_y).

Currently, there is no existing research that explicitly states the full procedure for gathering oscillatory rheological data on highly loaded suspensions that approach the maximum packing fraction. Existing research is largely confined to viscometric measurements [9-11] that are non-transferrable due to geometries used, generally cone and plate [18] which has an exceedingly small gap that is not conducive to testing with particles in excess of 10micron, or the incorporation of pre-shear stages [9,13,18,20,21] which leads to sample exudation from the gap for highly loaded systems. There are reports regarding highly loaded suspensions that provide oscillatory rheology data, either amplitude or frequency sweeps, but these reports either provide data without any mention of experimental procedure or only provide a passing statement regarding their procedure [8-25] . The closest existing research in the literature is for cement pastes [24] but the material analyzed doesn't approach the volume fractions in question here and thus can only be partially relied upon.

Herein, a procedure specifically developed to measure data for highly loaded suspensions tested in an oscillatory rheometer will be described in step-by-step fashion and data provided to illustrate its utility. This report is intended as the opening of the conversation regarding the complexity of this method of measurement, not its conclusion. The proposed procedure is the beginning of an effort to establish best practices for measuring highly loaded suspensions using oscillatory rheometry.

2. Materials and Methods

2.1. *Materials*

Rheometer: The procedures described in this report were developed on a Netzsch Kinexus Ultra+ stress-controlled rheometer. 20mm cross-hatched plates, upper and lower, were used to gather data. Hatches were approximately 1x1x1mm pyramids. A gap between 1.8 and 2.2mm was used in all experiments. The maximum axial force applicable by this instrument is 20N. The instrument was kept at 20C for all testing. The instrument room was also kept at 20C for all testing. Humidity was not tracked or controlled.

Mixer: A FlackTek SpeedMixer (DAC 1200-300 VAC) was used to mix the samples. 50g mixes were performed in a 90mL cup with rounded corners.

Filler: Coarse (D50 – 86 µm) and fine (D50 – 14.5 µm) melamine were used as the filler material for these experiments. Both particle sizes of melamine were sourced from OCI Nitrogen. For the coarse particles used the 90th percentile diameter was 180 µm. Thus, the gap used in rheometry should be 1.8mm or larger (gaps of this size are not reasonably attainable on cone and plate test geometries). All mixes were performed with a 3:1 ratio of coarse to fine particles to attain maximum packing density. The particle size distribution for the material is shown below in figure 1

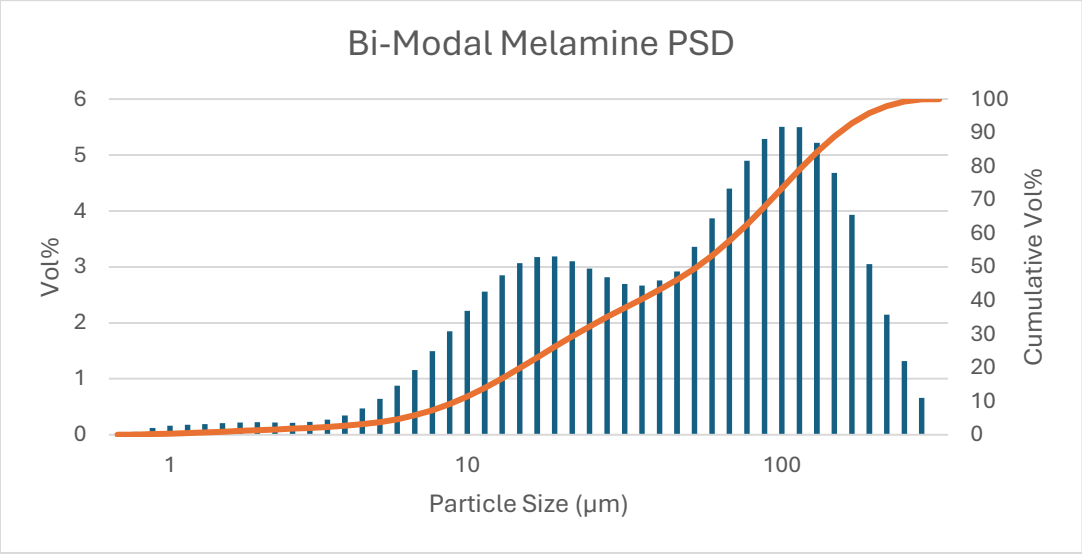

Figure 1: Melamine Particle Size Distribution, Coarse and Fine

Binder: Two binders were used in sample preparation, SYLGARD 182 and a custom methacrylate binder. SYLGARD 182 (part A), from DOW, has a density of 1.03g/cc and a neat binder viscosity of 5.5 Pa-sec. The custom binder has a density of 1g/cc and a neat binder viscosity of 0.35 Pa-sec.

Test Samples: The mixed material was allowed to cool to room temperature for 1 hour then formed into 3g spheres. Spherical test samples were allowed to relax overnight in the same room as the instrument before being tested.

Scale: A Mettler Toledo ME-T scale with +/- 0.001g sensitivity and 260g max was used to formulate each batch and weigh out test samples into spheres.

2.2. *Rheological Measurements*

2.2.1. *Existing Procedures*

Traditional procedures for gathering rotational rheology data rely heavily on pre-shearing the sample for a pre-determined time, then allowing the sample to dwell for a set time thereafter. For example, a sample could be pre-shear at 1 sec^{-1} for 120 seconds and then allowed to rest for 120 seconds before proceeding with the test. This is done to start each test from the same material condition, and thus obtain the same result. The assumption here is that the material is sheared to breakdown its internal structure entirely and then allowed to rest for that structure to recover to a consistent point. For non-filled, or lightly-filled, systems this process generally works very well

[9,13,18,20,21]. This, however, does not work for highly loaded suspensions due to sample exudation at high shears. When sheared at rates close to 1 sec^{-1} highly loaded suspensions will either flow out of the gap or separate from the top or bottom plate and render the test invalid as shown in figure 2.

Figure 2: Flow Out of Gap During Test

2.2.2. *Developed Procedure*

This report will detail procedures for two different classes of material, viscoelastic liquids and viscoelastic solids. The difference between these materials is highlighted by their recovery after a step strain is imposed and subsequently removed. A viscoelastic liquid will recover slowly, but incompletely, whereas a viscoelastic solid will recover quickly and completely [5,6]. The viscoelastic liquid was a formulation of 78vol% melamine (3:1 coarse: fine) in a custom binder and the viscoelastic solid was a formulation of 78vol% melamine in SYLGARD 182. Images of each formulation are shown below in figure 3 a-b.

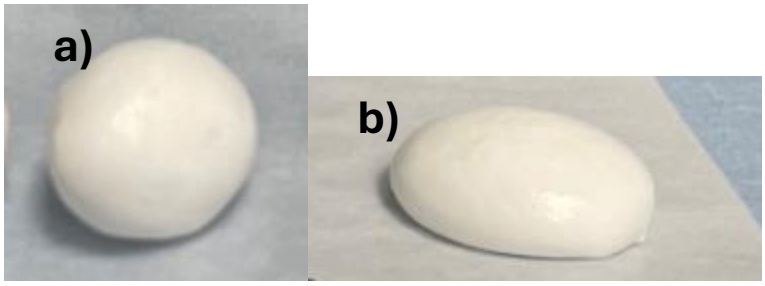

Figure 3 a-b Preformed Samples after 12 Hours Resting a) 78vol% SYLGARD, viscoelastic solid b) 78vol% Custom Binder, viscoelastic liquid

At the beginning of each day the top and bottom plates were cleaned using IPA. Additionally, gap zeroing, geometry inertia and torque mappings were performed. After each test the plates were cleaned again using IPA and water, then dried, and the gap zeroed anew. From this point the below descriptions start.

2.2.2.1. *Viscoelastic Liquid (VEL)*

Starting with the top plate at the loading gap (70mm) a 3g pre-formed sample was loaded onto the bottom plate. The top plate was then lowered to the trimming gap, 5% above the testing

gap, and the excess sample trimmed. After trimming the upper plate is brought down to the testing gap in a loop consisting of two steps. First, the top plate is lowered one tenth of the distance to the testing gap, then a small strain oscillation (5E-4%, 1Hz) is conducted for 180sec to dissipate normal force and promote plate-material adhesion. This loop is repeated until the testing gap is reached. Upon reaching the testing gap a series of low amplitude stress oscillations (1Pa, 1Hz) were performed for 15min to further promote plate adhesion. After 15min the test begun.

2.2.2.1.1. Assessing Plate Adhesion for Viscoelastic Liquids

Plate adhesion for viscoelastic liquids can be assessed by performing subsequent amplitude sweeps and comparing results. However, doing so while comparing different loading procedures consumes excess resources – both material and time. Thus, a good heuristic for assessing plate adhesion can be simply pulling the plates apart after loading and observing how the material behaves. For this procedure, the testing gap was 2mm. After loading, the gap was opened to 10mm to assess initial material breakup and plate adhesion, then further to 25mm to assess full material breakup. Good plate adhesion was regarding as uniform necking of material towards the central vertical axis when the plate was initially moved to 10mm, as shown in figure 4-b, followed by the formation of axially symmetric peaks at 25mm, as shown in figure 4-c. Bad plate adhesion resulted in material breaking away from specific points on the test geometry and asymmetry in the sample after plate pull-off. This procedure was tuned initially through this heuristic, then verified against the statistical profile of the data collected as will be shown later in this report.

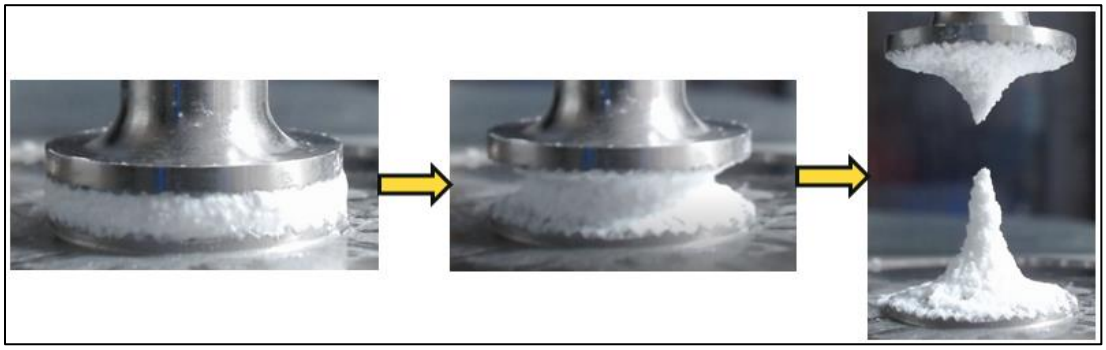

Figure 4 a-c: Viscoelastic Liquid, Desirable Plate Adhesion

2.2.2.2. <u>Viscoelastic Solid (VES)</u>

Upon starting the test, the instrument was brought to the loading gap (70mm) and a 3g pre-formed sample was loaded onto the bottom plate. The top plate was lowered to the trimming gap, 2.1mm, which the instrument was unable to reach. For this reason, it was required to move to an intermediate trimming gap twice the testing gap, or 4mm, then attempt to move down to the trimming gap. After 30s of attempting to move to the trim gap, a low strain oscillation (5E-4%, 1Hz) was be performed for 30s. Then the top plate was raised back to the intermediate gap. This was done until the trim gap was reached. Upon reaching the trimming gap, the sample is trimmed, then the same procedure is repeated to move from the trimming gap to the testing gap – only with the intermediate gap now set at 15% higher than the trimming gap (2.3mm).

Upon reaching the testing gap a series of low amplitude stress oscillations (1Pa, 1Hz) were performed for 15min to further promote plate adhesion. After 15min the test begun.

2.2.2.2.1. (U) Assessing Plate Adhesion for Viscoelastic Solids

For viscoelastic solid materials the same evaluation criterion cannot be used as what is used for a viscoelastic liquid. With viscoelastic solids there will be no breakup of the sample between upper and lower plates, but the entire sample will stick to either the top or the bottom plate when they are slowly separated. Here, it is proposed that the sample should stick entirely to the top plate as a sign of good plate adhesion. An example of good plate adhesion, for an untrimmed sample, is shown below in figure 5.

Figure 5: *Viscoelastic Solid, Desirable Plate Adhesion*

2.2.2.3. Data Quality and Interpretation

In this report, the coefficient of variation (CoV) is used to interpret the quality of the data attained. The coefficient of variation is defined as the ratio between the standard deviation and average within a dataset, per equation (1).

$$\text{CoV} = \sigma \, / \, \mu \tag{1}$$

Where σ is the standard deviation of the population and μ is the average. For reporting purposes, 10% CoV is considered an acceptable amount of variation. Low variation in the data across the linear viscoelastic region (LVER) of an amplitude sweep suggests that each run has good plate adhesion and that the sample was not structurally recovering through the test. Further, each sample was visually inspected throughout the entirety of each run. For all tests there was no evidence of plate separation or binder filtration.

2.2.2.4. *Yield Stress Determination*

In all cases the yield stress is taken as the stress where the storage modulus drops to 90% of the linear storage modulus value for the run. This is depicted in an example in figure 6.

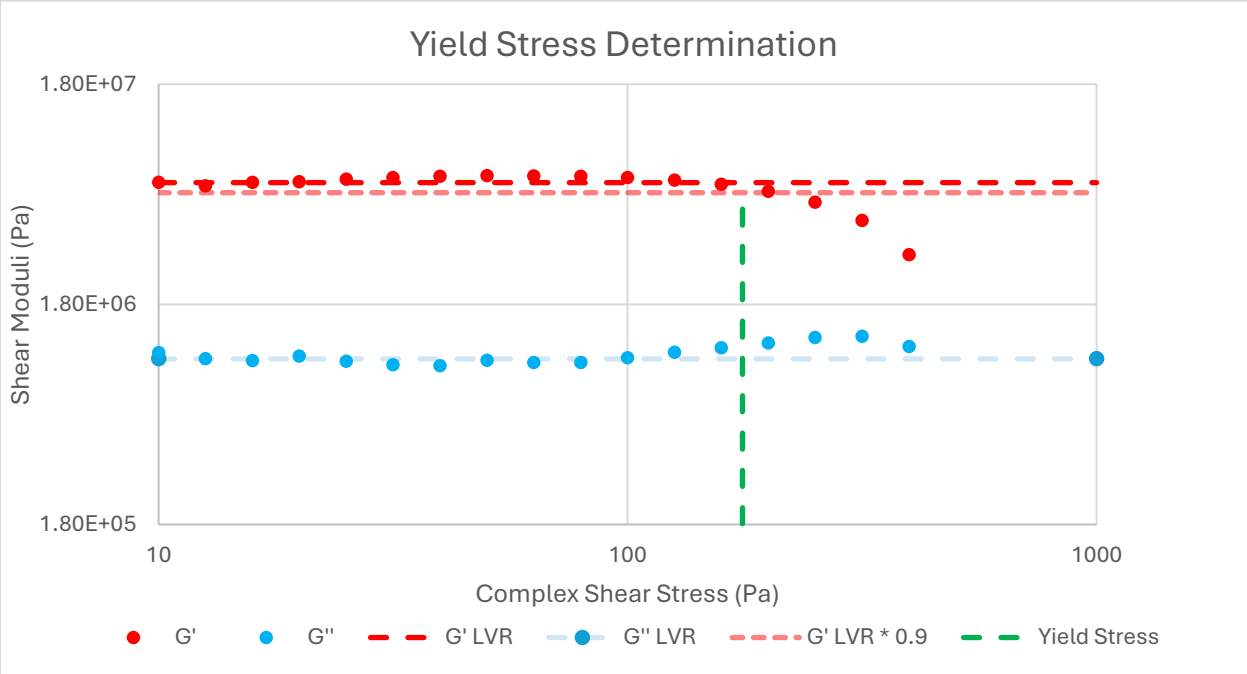

Figure 6: Example Yield Stress Determination

In the above graph, the darker red line is the linear storage modulus value. The light red line with smaller dashes is the moduli value corresponding with 90% of linear storage modulus. When the data crosses the 90% value, the yield stress value is taken. This is shown by the vertical green line.

3. Results and Discussion

3.1. Amplitude Sweep: Moduli Analysis

Amplitude sweeps were performed at 1Hz for both sample classes after using the proposed loading procedures detailed above. The amplitude sweep started at 10Pa and proceeded until the moduli crossed over. The results gathered are shown below in figure 7.

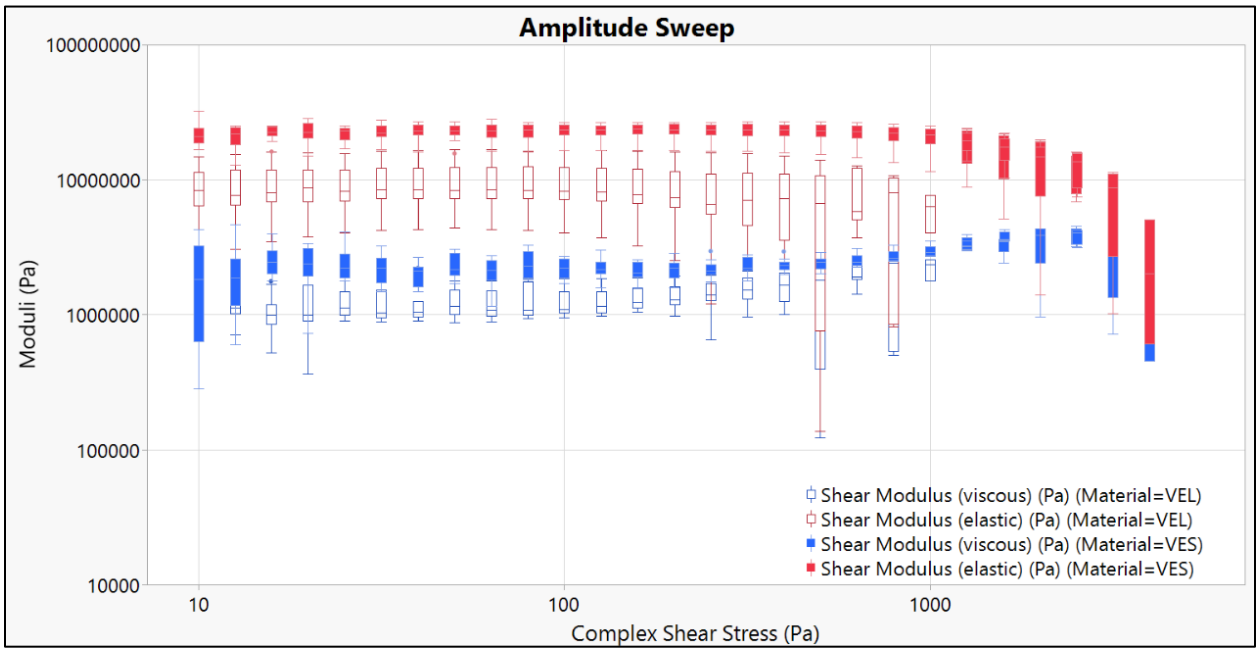

Figure 7: Amplitude sweep for two highly loaded suspension formulations
Solid boxes show viscoelastic solid data, hollow boxes show viscoelastic liquid data; storage modulus shown in red, loss modulus shown in blue

Both samples behave as expected, with a consistent linear trend at low stresses that breaks down as the stress increases beyond a certain point, or yield stress. When collating data from many runs there is a degree of spread in the dataset that must be characterized to determine if we can accept the data and take the average values in the linear viscoelastic region as accurate.

The degree of spread is conveyed via the coefficient of variation across the stress range, as shown in figure 8.

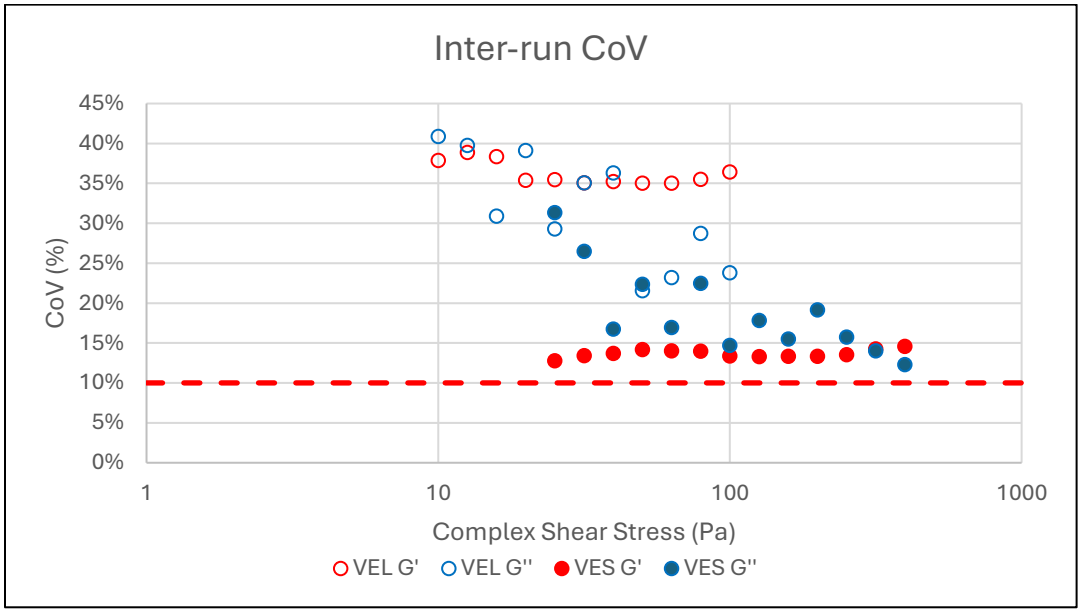

Figure 8: Inter-run Coefficient of Variation (CoV) for viscoelastic liquid and solid, storage and loss modulus.

As defined earlier, 10% CoV is taken as the threshold that must be cleared for data to be deemed acceptable. For both materials, and both moduli, the 10% threshold is not cleared. Therefore, the average values in the linear viscoelastic region for the storage and loss modulus cannot be taken as the actual values.

With the inter-run CoV determined to be too high the intra-run CoV must be investigated to deem if the data is at all acceptable with this testing procedure as prescribed. The intra-run CoV is shown in figure 9.

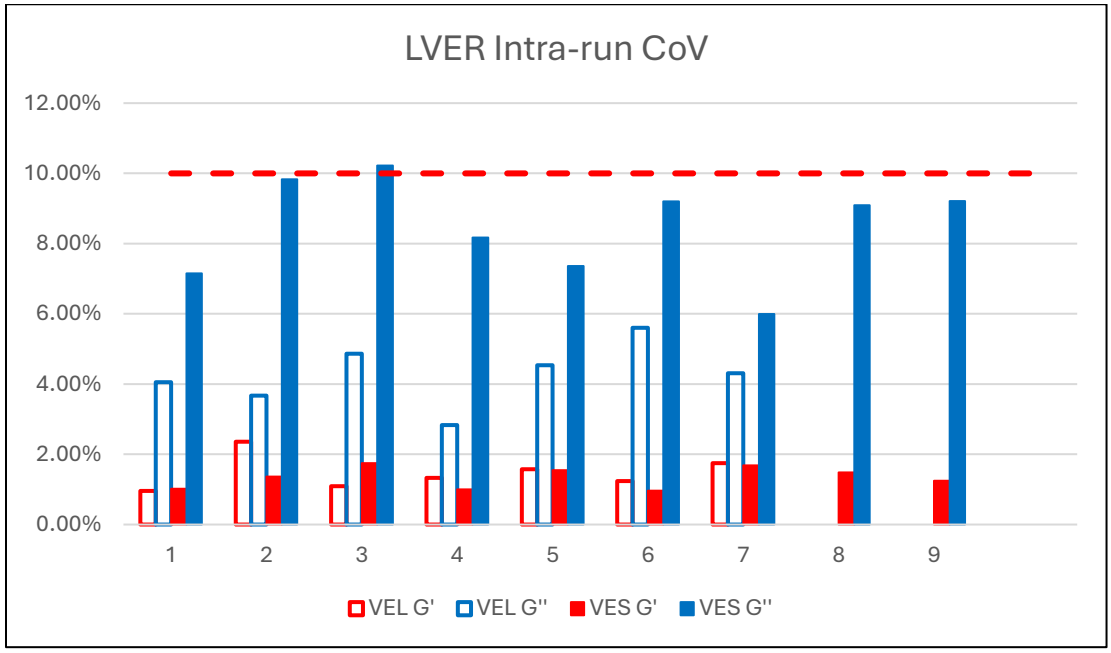

Figure 9: Intra-Run CoV for Viscoelastic Liquid (hollow) and Viscoelastic Solid (solid), Storage Modulus (Red) and Loss Modulus (Blue). LVER for VEL: 20-100Pa, VES: 20-400

The intra-run CoV shows that, aside from the loss modulus in one run for the viscoelastic liquid sample, all runs were of sufficient quality to have their individual data accepted. It is especially clear that for all samples the CoV of the storage modulus was very low, only exceeding 2% in one run. With the disparity between the inter and intra-run CoV in view, it is supposed that there is an additional factor contributing to variation between runs.

It is hypothesized that the additional contributing is the retained normal force from sample loading. When performing the loading procedure as proposed here there is a certain amount of force required to drive the sample into the teeth of the test geometry and attain a test gap that enables testing. If the sample were not properly adhered to the test apparatus, or too large of a gap was left, the gathered results would be unacceptable and test failure, due to material exudation from the gap, would be frequent. Thus, the material must be properly forced into the gap and adhere to the test geometry. The test instrument imposes a certain amount of force, in this case up to 20N, to achieve this goal. When the sample has been compressed into the desired test state there remains residual stresses within the material due to the loading procedure. This can be measured by the retained normal force that is not dissipated before the start of the test. It is hypothesized that this retained normal force is causing the variation seen in the inter-run CoV data as seen in figure 8 above. This hypothesis is tested in figure 10 below and the results of two different types of model fitting shown in table 1.

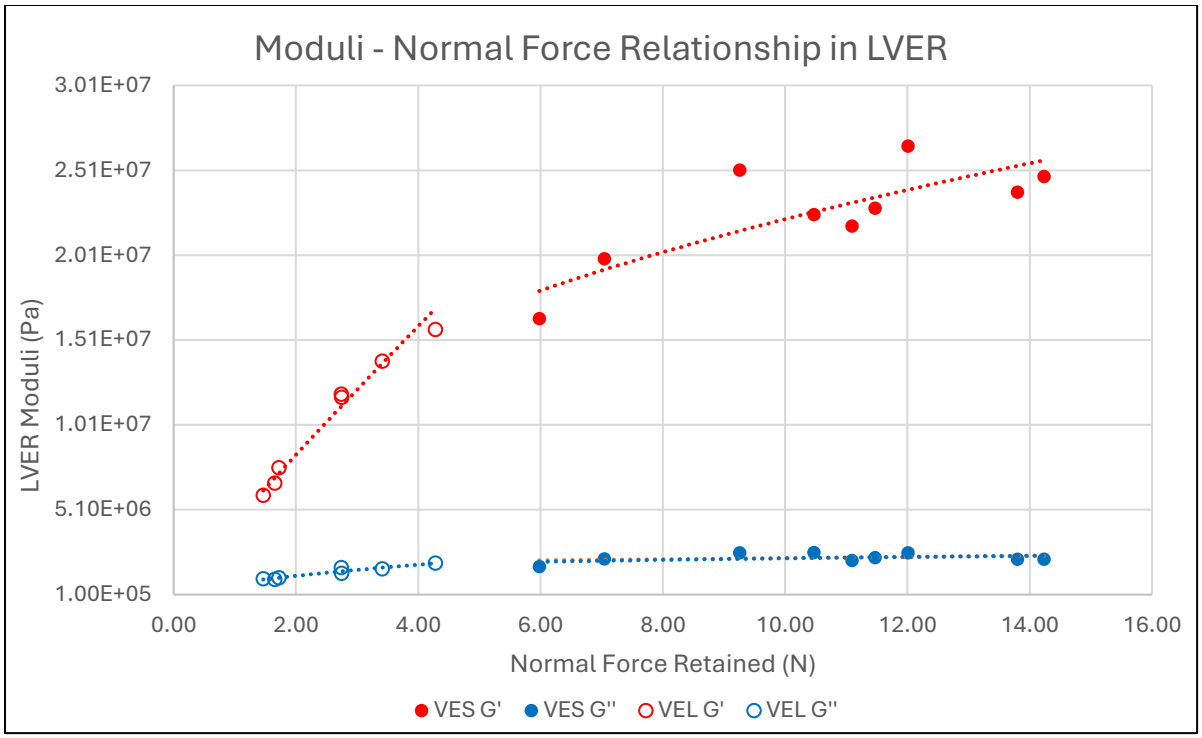

Figure 10: LVER Moduli v. Normal Force Retained for VEL (hollow) and VES (solid) samples Storage Modulus (red) and Loss Modulus (Blue)

Each point in figure 10 above represents a different test where a new sample was loaded with the same prescribed procedure and the retained normal force at the start of the test allowed to vary freely. The linear storage and loss modulus are taken as the average value of the modulus in the LVER. For the VEL this was range was 20-100 Pa and for the VES this was 20-400 Pa.

Figure 10 shows the normal force value at the beginning of the test against the LVER moduli measured in that test. All material-property pairings exhibit clear qualitative correlation. The correlation is explored quantitatively in table 1 below.

Model			Material			
			VEL		VES	
			G'	G"	G'	G"
Linear	Summary of Fit	R^2	0.97	0.9	0.58	0.11
	Parameter Estimate	Intercept Value (Pa)	1.25E+06	5.10E+05	1.38E+07	1.93E+06
		Intercept P-value	0.1702	0.0135	0.002	0.0015
Power Law	Summary of Fit	R^2	0.98	0.92	0.68	0.21
	Parameter Estimate	Intercept Value (Pa)	4.37E+06	7.75E+05	8.69E+06	1.43E+06
		Intercept P-value	<0.0001	<0.0001	<0.0001	<0.0001

Table 1: Moduli-Retained Normal Force Model Fits and Values; full model fit available in appendix

Two models are shown above, a linear fit and power law fit. Both the storage and loss moduli are fit for both material classes in question. The overall correlation coefficient is given for each material-property pairing (i.e. VEL G'). Additionally, the intercept parameter estimate for each model is given along with its p-value, to communicate its statistical significance. The intercept is of interest as it represents the actual moduli, where no normal force is retained. For the linear model, the viscoelastic liquid is well fit for both the storage and loss modulus. However, the intercept value for the storage modulus is not statistically significant and is only weakly significant for the loss modulus. In this case, neither of these values would be interpreted as the 'true' moduli for a zero normal force retained scenario. The linear model for the viscoelastic solid has poor overall model correlation, as conveyed by R^2, but much better intercept parameter estimates, both of which are statistically significant. Both values can be taken as the true moduli, but if a better fit is present, it may be taken instead.

In all cases the power law fit appears as a better model for these material-property combinations. In all cases the power law fit has a higher correlation coefficient and a more statistically significant p-value for the intercept estimate. In all cases the p-value is less than 0.0001 indicating very convincing significance. With this information the hypothesis that retained normal force is impacting the measured moduli value can be accepted. Further, it can be concluded that the proper moduli value can be determined by performing a power law fit of the LVER moduli value from each run against the retained normal force at the start of the run and the extracted intercept value taken as the true LVER moduli.

Additionally, the hypothesis is logically justified because, when dealing with highly solids loaded suspensions approaching the maximum packing fraction, any retained normal force is going to directly lead to increased particle-particle interactions within the sample. These increased frictional interactions will form force chains that store energy, increasing the storage modulus, and further increase dissipative losses through sliding interactions, increasing the loss modulus.

3.2. *Yield Stress Analysis*

A similar analysis can be performed for the yield stress determined for each run via the procedure shown in section 2.2.2.4. It is hypothesized that the yield stress will behave similarly to the storage modulus: additional stress will be withstood when the material is tested under compression. The results of testing are shown in figure 11 below.

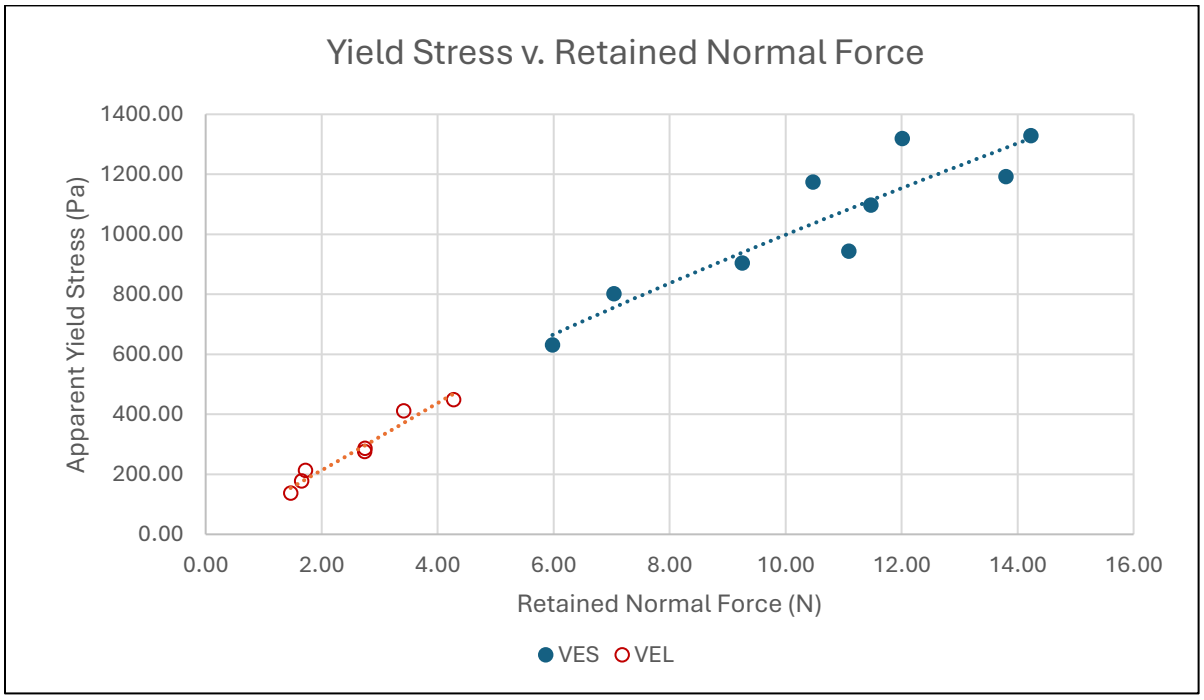

Figure 11: Yield Stress v. Retained Normal Force; Viscoelastic Solid (blue, solid) and Viscoelastic Liquid (orange, hollow)

There is an apparent correlation between the yield stress from each run and the normal force at the beginning of the test. Again, two models are fit to the data to observe if statistically significant intercept values may be extracted that can be interpreted as true yield stress values for each material class. This data is shown in table 2 below.

Model			Material	
			VEL	VES
			Yield Stress	Yield Stress
Linear	Summary of Fit	R^2	0.95	0.82
	Parameter Estimate	Intercept Value (Pa)	-3.02E+00	2.21E+02
		Intercept P-value	0.92	0.18
Power Law	Summary of Fit	R^2	0.95	0.87
	Parameter Estimate	Intercept Value (Pa)	1.04E+02	1.61E+02
		Intercept P-value	< 0.0001	< 0.0001

Table 2: Yield Stress v. Retained Normal Force Model Fits, Linear and Power Law

As was the case with the moduli and retained normal force, again the power law fit proves to be superior to the linear fit. In both material cases, the power law fit has an equal or higher correlation coefficient and more statistically significant intercept parameter estimates. For both materials the intercept value is very statistically significant. With this in view we can accept the intercept estimates from the power law fit as the yield stress values for these materials.

4. Conclusion:

In this report procedures were set forth for measuring critical rheological properties – linear storage modulus, linear loss modulus, and yield stress – of highly solids loaded suspensions of two different classes: viscoelastic liquids and viscoelastic solids. Each procedure was tailored to attain sufficient plate adhesion, at a reasonable test gap, to enable successful testing across a range of shear stresses without sample exudation, edge fracture, or binder filtration. In the process of establishing these procedures a fundamental tradeoff between plate adhesion and data quality was uncovered. It was shown that in pursuit of attaining acceptable plate adhesion compressive stresses, measured by the retained normal force, were carried into the subsequent experiment; and, that the retained normal force does impact the measured values of each desired characteristic rheological property. It was then hypothesized that the retained normal force varies *predictably* against the desired rheological properties and models can be fit to predict the values of these desired properties at conditions with no normal force retained. This hypothesis was confirmed when statistically significant power-law relationships were established for all rheological properties of interest for both material classes. Using these relationships model intercept values, corresponding to the zero retained normal force condition, were extracted and interpreted as the actual property value. In all cases the intercept values were statistically significant with p-values less than 0.0001. With this hypothesis confirmed the proposed testing procedures, to include power-law model fitting, are shown to be the first open publication of complete oscillatory rheometry testing procedures for highly solids loaded suspensions that can obtain linear storage modulus, linear loss modulus, and yield stress data.

Funding Statement: *This research did not receive any specific grant from funding agencies in the public, commercial, or not-for-profit sectors.*

Data Availability: *The raw data required to reproduce the above findings cannot be shared at this time as the data also forms part of an ongoing study.*

References:

1. Marnot, A., Dobbs, A. & Brettmann, B. Material extrusion additive manufacturing of dense pastes consisting of macroscopic particles. *MRS Communications* **12**, 483–494 (2022). https://do-i.org/10.1557/s43579-022-00209-1
2. Ewoldt, R.H., M.T. Johnston, L.M. Caretta, "Experimental challenges of shear rheology: how to avoid bad data," in: S. Spagnolie (Editor), Complex Fluids in Biological Systems, Springer (2015) http://dx.doi.org/10.1007/978-1-4939-2065-5_6
3. He, J., Lee, S.S., Kalyon D.M., Shear viscosity and wall slip behavior of dense suspensions of polydisperse particles . *J. Rheol.* 1 January 2019; 63 (1): 19–32. https://doi.org/10.1122/1.5053702
4. Cloitre, M., Bonnecaze, R.T. A review on wall slip in high solid dispersions. *Rheol Acta* 56, 283–305 (2017). https://doi.org/10.1007/s00397-017-1002-7
5. Morrison, Faith A. *Understanding Rheology*, Oxford University Press, 2001
6. MACOSKO C. W. *Rheology Principles, Measurements and Applications*, VCH Publishes, 1994
7. Kalyon, Dilhan M., Aktaş, Seda, *Factors Affecting the Rheology and Processability of Highly Filled Suspensions*, 2014, Annual Review of Chemical and Biomolecular Engineering, Volume 5, 2014, 229-254, 1947-5446, https://doi.org/10.1146/annurev-chembioeng-060713-040211
8. Kaully, T., Siegmann, A. and Shacham, D. (2007), Rheology of highly filled natural CaCO3 composites. II. Effects of solid loading and particle size distribution on rotational rheometry. Polym Compos, 28: 524-533. https://doi.org/10.1002/pc.20309
9. Ferraris, C.F., (1999), Measurement of the rheological properties of cement paste: a new approach. Role of Admixtures in High Performance Concrete, RILEM International Symposium. Proceedings.
10. Kalyon DM, Yaras P, Aral B, Yilmazer UY. 1993. Rheological behavior of a concentrated suspension: a solid rocket fuel simulant. J. Rheol. 37:35–53
11. Feger C, Gelorme JD, McGlashan-Powell M, Kalyon DM. Mixing, rheology,and stability of highly filled thermal pastes. IBM J Res Dev 2005;49:699–707
12. Chae DW, Kim BC. Thermal and rheological properties of highly concentrated PET composites with ferrite nanoparticles. Compos SciTechnol 2007;67:1348–52
13. Ley-Herna´ndez AM, Feys D (2020) Challenges in Rheological Characterization of Cement Pastes Using a Parallel- Plates Geometry. In: Mechtcherine V, Khayat KH, Secrieru E (eds) Rheology and processing of construction materials, rheocon 2019/SCC9, RILEM Bookseries 23. Springer, Cham, pp 228–236
14. Vance, K., Sant, G., Neithalath, N., The rheology of cementitious suspensions: A closer look at experimental parameters and property determination using common rheological models, Cement and Concrete Composites, Volume 59, 2015, Pages 38-48, ISSN 0958-9465, https://doi.org/10.1016/j.cemconcomp.2015.03.001
15. Ferraris CF, Geiker M, Martys NS et al (2007) Parallel-plate rheometer calibration using oil and computer simulation. J Adv Concr Techn 5(3):363–371

16. Haist, M., Link, J., Nicia, D. et al. Interlaboratory study on rheological properties of cement pastes and reference substances: comparability of measurements performed with different rheometers and measurement geometries. Mater Struct 53, 92 (2020). https://doi.org/10.1617/s11527-020-01477-w
17. A. Ya. Malkin, A. V. Mityukov, S. V. Kotomin, A. A. Shabeko, V. G. Kulichikhin; Elasticity and plasticity of highly concentrated noncolloidal suspensions under shear. *J. Rheol.* 1 March 2020; 64 (2): 469–479. https://doi.org/10.1122/1.5115558
18. K. van der Vaart, Yasser Rahmani, Rojman Zargar, Zhibing Hu, Daniel Bonn, Peter Schall; Rheology of concentrated soft and hard-sphere suspensions. *J. Rheol.* 1 July 2013; 57 (4): 1195–1209. https://doi.org/10.1122/1.4808054
19. Mityukov, A.V.; Govorov, V.A.; Malkin, A.Y.; Kulichikhin, V.G. Rheology of Highly Concentrated Suspensions with a Bimodal Size Distribution of Solid Particles for Powder Injection Molding. Polymers 2021, 13, 2709. https://doi.org/10.3390/polym13162709
20. Rohit Lade, Kailas Wasewar, Rekha Sangtyani, Arvind Kumar, Dilip Peshwe & Diwakar Shende (2021): Effect of aluminium nanoparticles on rheology of AP based composite propellant: experimental study and mathematical modelling, Molecular Simulation, DOI: 10.1080/08927022.2021.1891305
21. Nair SAO, Alghamdi H, Arora A, Mehdipour I, Sant G, Neithalath N. Linking fresh paste microstructure, rheology and extrusion characteristics of cementitious binders for 3D printing. J Am Ceram Soc. 2019; 102: 3951–3964. https://doi.org/10.1111/jace.16305
22. Avery, Michael P., et al. "The rheology of dense colloidal pastes used in 3D-printing." Nip & digital fabrication conference. Vol. 30. Society for Imaging Science and Technology, 2014.
23. Sweeney, M.A., Bratton, K.R., Woodruff, C., Cagle, C., Hill, K.J., Pantoya, M.L. and Christopher, G.F. (2019), Effects of Shear Rate during Energetic Material Processing on Reactivity. Adv. Eng. Mater., 21: 1801324. https://doi.org/10.1002/adem.201801324
24. Fábio A. Cardoso, Alessandra L. Fujii, Rafael G. Pileggi, Mohend Chaouche, Parallel-plate rotational rheometry of cement paste: Influence of the squeeze velocity during gap positioning, Cement and Concrete Research, Volume 75, 2015, Pages 66-74, ISSN 0008-8846, https://doi.org/10.1016/j.cemconres.2015.04.010.
25. TA Instruments, Normal force measurements on the AR 1000-N Rheometer PART II,(2005), http://www.tainstruments.com/2005.; accessed 4 OCT 2024
26. Mendes, Paulo R. de Souza, Alicke, Alexandra A. and Thompson, Roney L.. "Parallel-Plate Geometry Correction for Transient Rheometric Experiments" Applied Rheology, vol. 24, no. 5, 2014, pp. 1-10. https://doi.org/10.3933/applrheol-24-52721
27. Erol, M. and Kalyon, D. M.. "Assessment of the Degree of Mixedness of Filled Polymers: Effects of Processing Histories in Batch Mixer and Co-Rotating and Counter-rotating Twin Screw Extruders" *International Polymer Processing*, vol. 20, no. 3, 2005, pp. 228-237. https://doi.org/10.3139/217.1882
28. Illowsky, Barbara, and Susan L Dean. *Introductory Statistics*. Houston, Texas, Openstax, Rice University, 2017.
29. Romberg, Stian K., "Structural stability of thermosets during material extrusion additive anufacturing. " PhD diss., University of Tennessee, 2021. https://trace.tennessee.edu/utk_graddiss/6984
30. Cohesive vs. adhesive failure in adhesive bonding (biolinscientific.com), accessed 4 OCT 2024
31. shop.nist.gov/ccrz__ProductDetails?sku=2492&cclcl=en_US, accessed 4 OCT 2024